Open Access Online Journal on Astronomy and Astrophysics

Acta Astrophysica Taurica

www.astrophysicatauricum.org

Acta Astrophys. Tau. 5(4), 29–34 (2024)

Circular polarization of millimeter emission from solar flares

V. Ryzhov[1], P. Shivrina[1], V. Smirnova[2]

[1] Bauman Moscow State Technical University, 2nd Baumanskaya 5, Moscow 105005, Russia
[2] Crimean Astrophysical Observatory, Nauchny 298409
e-mail: vvsvid.smirnova@yandex.ru

Received 30 October 2022

ABSTRACT

We present new observations of circular polarization of solar flares observed with the Bauman Moscow State Technical University radio telescope RT-7.5 at a frequency of 93 GHz. Time profiles of the right and left circular polarization intensity of radio emission obtained for several flare events are analyzed. It was shown that the upper limit of the degree of circular polarization for the maximum phase of the studied flares is ~5%.

Key words: Sun, radio emission, polarization of millimeter emission, polarization receiver

1 Introduction

The RT-7.5 radio telescope of the Bauman Moscow State Technical University is the only domestic radio telescope operating in the short-wave part of the millimeter (mm) wavelength range. It is equipped with a fully steerable reflector antenna with a primary mirror diameter of 7.75 m. Currently, the RT-7.5 radio telescope uses a dual-band receiver with operating frequencies of ν_1 = 93 GHz and ν_2 = 140 GHz for solar observations (Smirnova et al., 2017). The antenna beamwidth, which determines the angular resolution for these frequencies, is about 3 arcmin, and the pointing accuracy to the source is ~10″. These characteristics of the radio telescope allow observations in two modes: two-dimensional scanning of the Sun with the antenna beam, which yields a map of the brightness temperature distribution of radio emission over the solar disk, and long-term tracking of a selected active region with continuous recording of the signal from it (Tsap et al., 2018).

To date, there is very little information worldwide about the degree of polarization of solar flare emission in the mm range. To fill this gap, a 93 GHz polarization receiver was installed on the RT-7.5 radio telescope for the first time in 2021, providing conditions for studying the circular polarization of solar radio emission.

The purpose of this work is to test a new circular polarization separation scheme for the standard 93 GHz radiometer installed on the Bauman Moscow State Technical University radio telescope, as well as to accumulate statistics on the degree of circular polarization of mm radio emission from solar flares.

2 Operating modes of RT-7.5

The main operating mode of RT-7.5 is regular two-dimensional mapping of the entire solar disk. Most of the observations are conducted simultaneously at two frequencies: 93 and 140 GHz (3.2 and 2.2 mm bands).

Another mode of solar observations at RT-7.5 is tracking a single selected active region with a high flare development forecast for the entire possible observation time with the antenna beam. This mode allows obtaining flare intensity profiles at two frequencies with a maximum time resolution of 0.125 s. The mode is used when there is a high probability of a powerful flare developing in a single active region on the disk.

The polarization receiver, shown in Fig. 1, consists of a horn feed that receives mm emission; a polarizer that converts left and right circular polarization into corresponding linear polarization: vertical and horizontal; a polarization selector that separates vertical and horizontal polarization into separate channels. Next are modulators that alternately open the polarization channels. From the modulator outputs, the signals go through a totalizer to the standard thermostated 93 GHz radiometer. A feature of the receiver is obtaining data on the emission intensity of two types: at the right polarization and the difference in intensities at the right and left polarizations. However, due to the inequality of the transmission coefficient in the two channels, it was not possible to realize a “pure” difference in the intensities of the two polarizations in practice, and one of the polarizations prevails on the maps of the second type.

3 Method for estimating the degree of polarization

For this receiver, the following method for estimating the degree of polarization was developed. First, the continuous mapping of the full disk is performed with a “comb scan” with sequential acquisition of intensities I_1 and I_2 for each passage of the antenna beam:

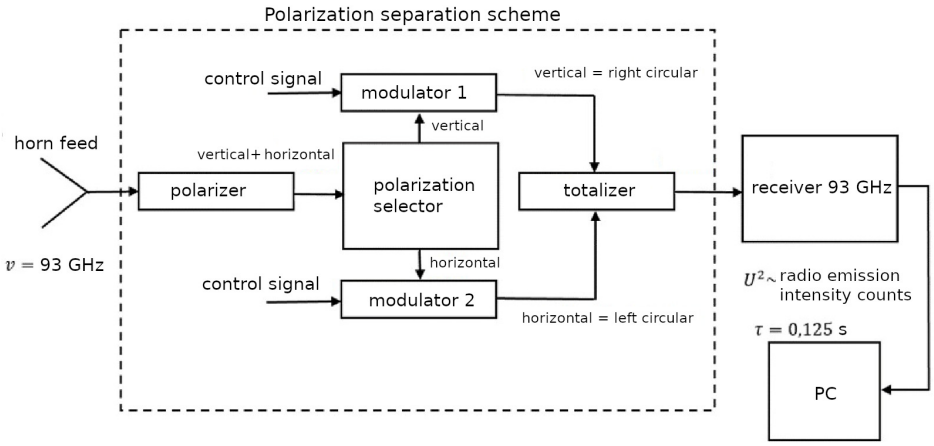

Fig. 1. Design of the 93 GHz polarization receiver.

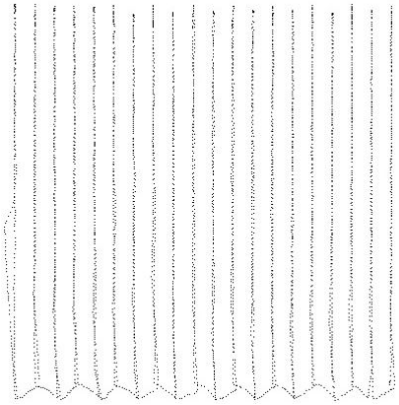

Fig. 2. Beam trajectory.

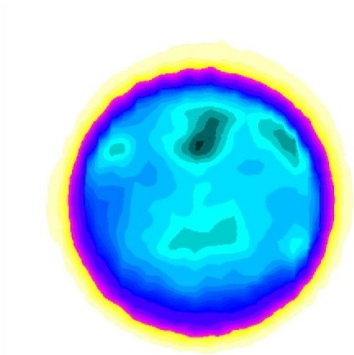

Fig. 3. Beam moving upward, right polarization.

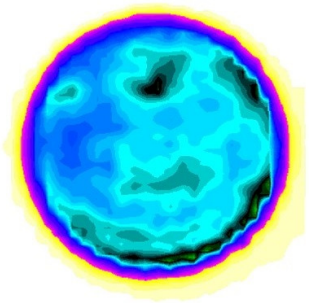

Fig. 4. Beam moving downward, polarization difference.

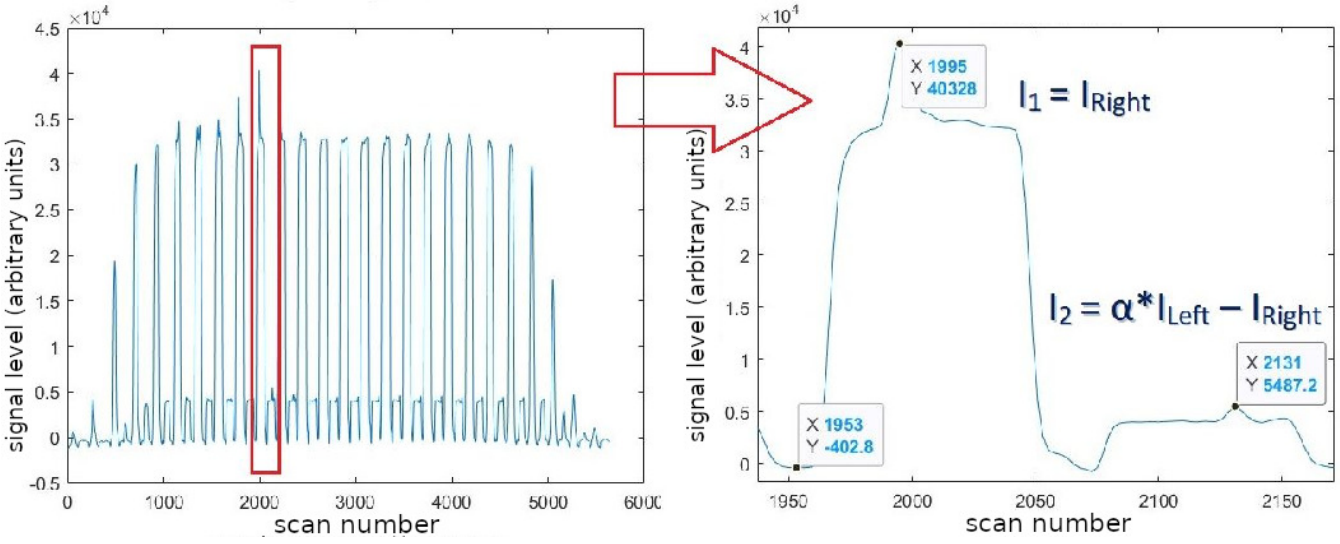

Fig. 5. Selection of the required scan line.

Table 1. Error budget for estimating the degree of polarization.

Error component name	Error type	Value	Note
caused by the system's own noise, right polarization	random, SD	0.03%	system fluctuation sensitivity $\Delta T_r = 1K$
caused by the system's own noise, difference channel	random, SD	0.2%	system fluctuation sensitivity $\Delta T_r = 1K$
caused by fluctuations of losses in the atmosphere	random, SD	1.6%	clear weather, fluctuation SD $\delta = 2\%$
caused by coordinate noise	random, SD	3.2%	wind speed less than 10 m/s, scanning error SD $\sigma_c = 5$ arcsec
caused by nonlinearity of the receiving path	uncompensated, systematic, limit	1.6%	receiving path nonlinearity $\delta_r = 7$ % (0.3 dB) within the antenna temperature dynamic range $T_A = 0 \ldots 1.5\,T_S$, where T_S is the antenna temperature when pointing to the center of the solar disk
caused by inter-channel delay	uncompensated, systematic, limit	3%	inter-channel delay $\Delta\tau = 24$ s, flare front duration $\tau_f = 300$ s
Resulting root-mean-square error in estimating the degree of polarization $\varepsilon_\Sigma = 4\%$			

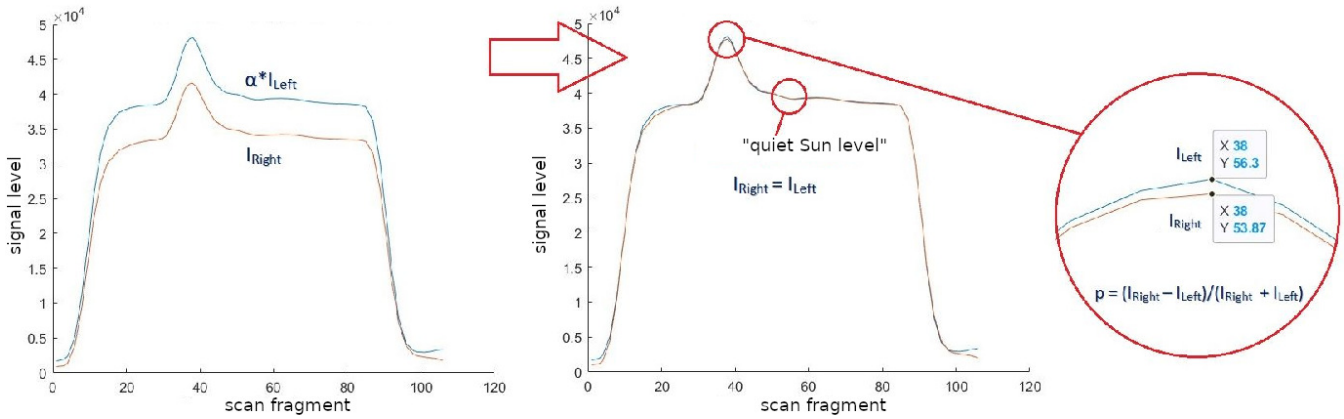

Fig. 6. Calibration and estimation of the degree of polarization.

$$I_1 = I_{\text{Right}} \tag{1}$$

$$I_2 = \alpha \times I_{\text{Left}} - I_{\text{Right}}. \tag{2}$$

Next, calibration is performed and the imbalance coefficient of the polarization separation scheme channels p is determined when observing the "quiet Sun" and "sky background" regions for which the degree of polarization is assumed to be $p = 0$:

$$I_{\text{Right}} = I_1 \tag{3}$$

$$I_{\text{Left}} = \frac{(I_1 + I_2)}{\alpha}. \tag{4}$$

Then, the degree of polarization is calculated using the formula

$$p = \frac{I_{\text{Right}} - I_{\text{Left}}}{I_{\text{Right}} + I_{\text{Left}}}. \tag{5}$$

The beam trajectory during the comb scan and examples of the obtained solar radio brightness maps are presented in Figs. 2–4 for two modes. At an angular scanning speed of 180 arcsec/s and a line length of $H = 40$ arcmin, the inter-channel response delay of the radiometer for the same point on the solar disk for the right polarization channel and the difference channel lies within $\Delta\tau = 4 \ldots 25$ s. The raster line step is $d = 2$ arcmin, and the total scanning duration, which determines the time resolution when estimating the degree of polarization, is $\tau_S \approx 10$ min. During post-processing data analysis, the line containing the largest response from the flare is determined (Fig. 5). Next, two adjacent scans are aligned

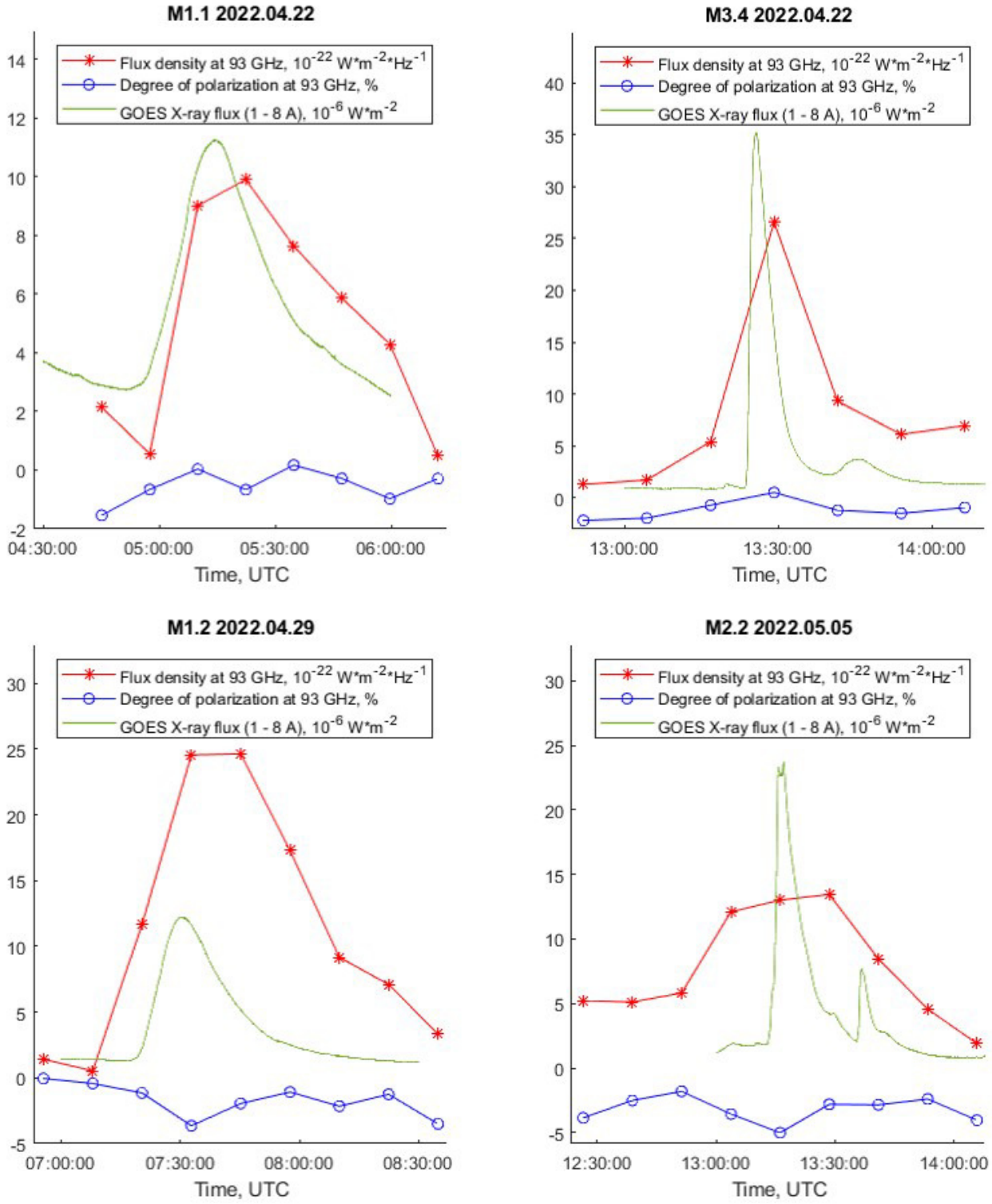

Fig. 7. Spectral flux density and degree of polarization of the recorded flares M1.1, M3.4 – 2022.04.22, M1.2 – 2022.04.29, M2.2 – 2022.05.05.

in time, as well as in the "quiet Sun" level with the determination of the imbalance coefficient α. After that, the maximum intensity values at the two polarizations are determined and the degree of polarization is calculated (Fig. 6).

The error in estimating the degree of polarization was found by statistical modeling with the determination of the value of each component separately. The error budget is presented in Table 1. Due to the proximity of the values of the

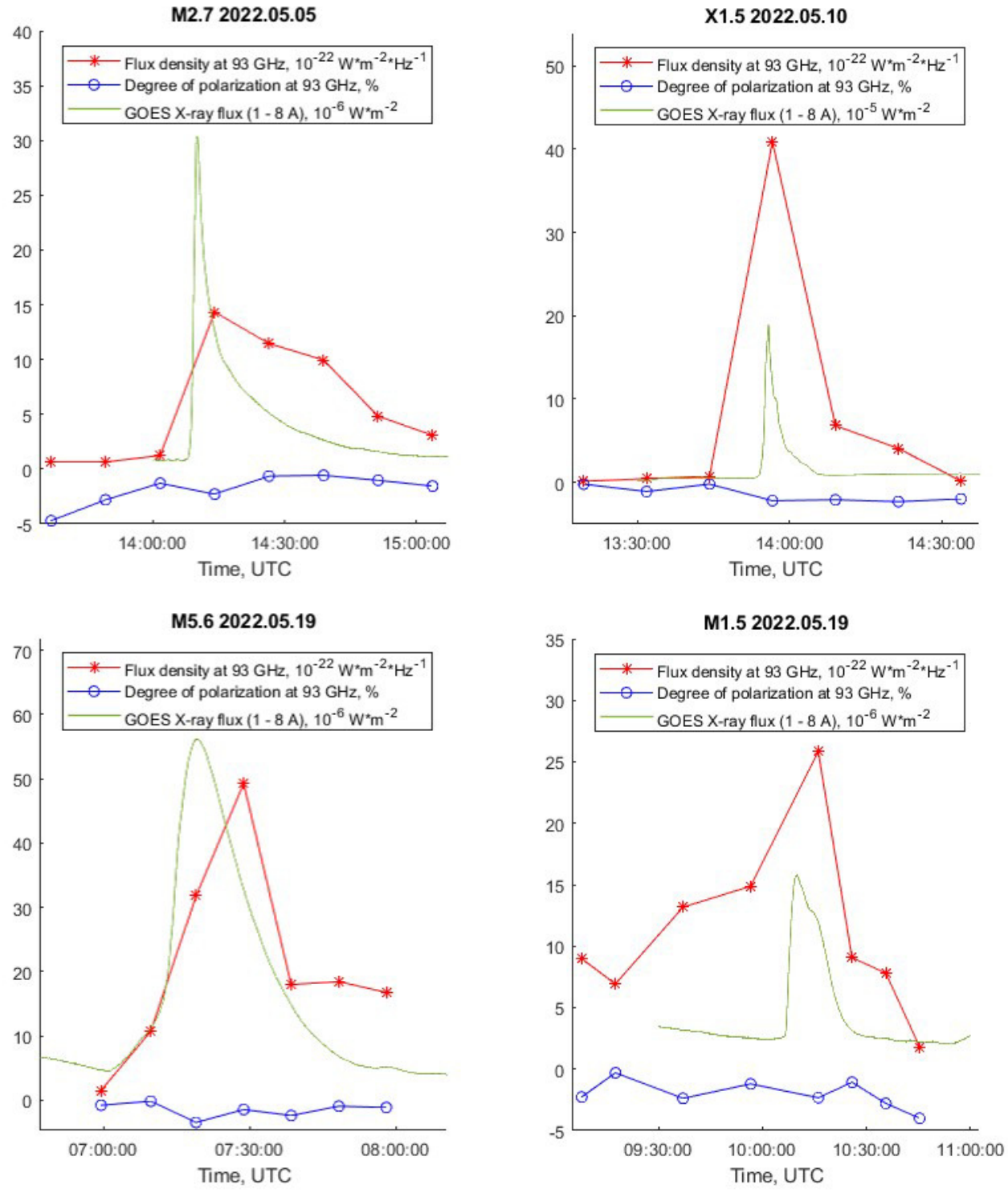

Fig. 8. Spectral flux density and degree of polarization of the recorded flares M2.7 – 2022.05.05, X1.5 – 2022.05.10, M5.6, M1.5 – 2022.05.19.

random components of the error and the uncompensated systematic ones, the latter were taken as random with standard deviations (SD) of 0.5 from their limits. The resulting root-mean-square error in estimating the degree of polarization was $\varepsilon_\Sigma = 4\%$.

In total, during the active observation period from 12.04.2022 to 23.06.2022, 51 flares occurred in the mapping intervals, of which 27 were C-class, 20 were M-class, and 4 were X-class flares. Using the presented method, an analysis was carried out for the eight most powerful M- and

Table 2. Statistics of recorded events.

Time, UTC	Class	Max SFD, 10^{-22} W × m^{-2}× Hz^{-1}	Min p,%	Max p,%
2022.04.22 04:52	M1.1	10 ± 2	−1.5 ± 4.0	0.2 ± 4.0
2022.04.22 13:16	M3.4	27 ± 5	−2.2 ± 4.0	0.5 ± 4.0
2022.04.29 07:15	M1.2	25 ± 5	−3.6 ± 4.0	0.0 ± 4.0
2022.05.05 13:08	M2.2	13 ± 3	−5.0 ± 4.0	−1.8 ± 4.0
2022.05.05 14:02	M2.7	14 ± 3	−4.8 ± 4.0	−0.6 ± 4.0
2022.05.10 13:50	X1.5	41 ± 8	−2.3 ± 4.0	−0.2 ± 4.0
2022.05.19 07:00	M5.6	49 ± 10	−3.4 ± 4.0	−0.2 ± 4.0
2022.05.19 10:00	M1.5	26 ± 5	−4.0 ± 4.0	−0.3 ± 4.0

X-class events; during their registration the lowest level of signal fluctuations was observed due to weather conditions. Figures 7 and 8 show the graphs of the recorded spectral flux density (SFD) at the right polarization, estimates of the degree of polarization, as well as the level of soft X-ray emission according to GOES data.

Table 2 presents the maximum SFD value of the flare at the right polarization, as well as the minimum and maximum values of the degree of polarization of the flare for the eight selected events.

4 Conclusions

In this work, new data on the degree of circular polarization of mm emission from solar flares were obtained. For all eight investigated M- and X-class events, the ratio of the measured absolute value of the degree of polarization to the root-mean-square error of the method (4%) during the flare development period did not exceed 1.25, which allows estimating the upper limit of the degree of polarization of mm emission from the considered events to be about 5%. Further optimization of the method, aimed at reducing each component of the error, will make it possible to increase the accuracy of the method to 2%. Our obtained upper estimate is significantly lower than that in other studies (Altyntsev et al., 2017; Silva, Valio, 2016). For further study of the proposed method, it is necessary to create a calibration source with a frequency of 93 GHz, which has a known and variable circular polarization and which can be placed in the far-field zone of the RT-7.5 radio telescope antenna.

This work was partially supported by the RFBR grant No. 20-52-26006 Czech Republic_a and the Ministry of Education and Science research project No. 1021051101548-7-1.3.8.

References

Altyntsev A., Meshalkina N., Myshyakov I., Pal'shin V., Fleishman G., 2017. Solar Phys., vol. 292, iss. 9, p. 137.

Silva D.F., Valio A.B.M., 2016. In Dorotovic I. et al. (Eds), Millimeter observation of solar flares with polarization. ASP Conf. Ser., San Francisco: ASP, vol. 504, p. 55.

Smirnova V.V., Tsap Yu.T., Shumov A.V., et al., 2017. Radiostroenie, no. 6, pp. 14–26. (In Russ.)

Tsap Yu.T., Smirnova V.V., Motorina G.G., et al., 2018. Solar Phys., vol. 293, no. 3, p. 50.